

# Kinematic Hybrid Position/Force Control Of a 3-DOF In-Parallel Actuated Manipulator

Patrick HUYNH  
Ngee Ann Polytechnic  
Mechanical Engineering Division  
535 Clementi Road, 599489 Singapore  
Email: huynh@np.edu.sg

**Abstract**—The paper aims to describe kinematic hybrid position/force control for a three-degree-of-freedom (3-DOF) in-parallel actuated manipulator, and its application to peg-in-hole task about 10 $\mu$ m clearance. The control system consists of a low-level position servo driven by force feedback in base coordinates. The computation required for the control is only inverse kinematics, which is very simple for the parallel-link manipulator. Assisted by a human operator, the motion is generated by using force-torque based joystick commands and/or preplanned motion data. In teleoperation mode, the human operator can intervene and superpose corrective motions over the preplanned searching motion.

**Keywords**—Parallel Manipulator; Kinematics; Hybrid position/force control; Teleoperation

## I. INTRODUCTION

During the past few years, there has been an increasing demand in the field of precision engineering for fine motion of multi-degrees of freedom. This motivates in the Mechanical Engineering Division at the Ngee Ann Polytechnic of Singapore the development of a new robotics application field, parallel mechanism. The choice of parallel structures for high precision applications is justified by numerous advantages:

- High stiffness and structural frequency.
- Precision.
- Mobility and compactness.
- Fixed actuators.
- Uniform distribution of the load.

However, the main disadvantage is a limited working space. The simplest way to cumulate precision and working volume consists in the utilization of a parallel manipulator combined with classic-serial robots, as the active wrist [1,2]. The parallel manipulator thus compensates the static errors of the sequential robot with serial structure. This principle is often described by the name “Macro-/mini-manipulator” [3].

Most researchers are concerned with the hybrid control of the 6-DOF parallel platform architecture; little work has been done on 3-DOF parallel-link manipulator force control. Merlet [4] worked on force-feedback control of parallel manipulators to get stable motion during assembly

tasks. Reboulet [2] developed hybrid control of a Stewart platform micro-manipulator mounted on a SCARA macro-manipulator to get overall system stability. By exploiting the advantage of parallel-links, Arai [5] implemented hybrid position/force control for a modified Stewart platform, assisted by human teleoperation via joystick, in order to show the good performance in application to peg-in-hole assembly with a 16 $\mu$ m clearance. Huynh and Arai [6] exploited that type of force-augmented control of the slave manipulator in their bilateral master-slave control scheme, to enable the stable contact between the slave parallel manipulator end-effector and the rigid environment.

In many respects, the paper focuses on the kinematic hybrid control of a 3-DOF linear type in-parallel actuated manipulator, which has been evolved from previous research studies [5-7] and experiences concerning parallel robotic platform manipulators at Stanford University, USA [1,8] and Mechanical Engineering Laboratory, Japan [9,11]. This type of parallel manipulator has been designed and fabricated in the Mechanical Engineering Division at the Ngee Ann Polytechnic of Singapore, and has the potential to produce high precision, an attribute desirable for a robot wrist.

In this paper, we first introduce briefly the geometric and kinematic models of the 3-DOF in-parallel actuated manipulator. Their detailed calculation has been reported in [11]. Then, the kinematic hybrid position/force control scheme is presented along with its hardware and software implementation. Finally, the applicability of the proposed control is shown in metal-to-metal contact and peg-in-hole task.

## II. 3-DOF IN-PARALLEL ACTUATED MANIPULATOR PROTOTYPE

### A. Kinematic Configuration

The prototype is a linear type 3-DOF parallel manipulator represented in Fig. 1. Its top view at initial position is illustrated in Fig. 2. It composes of a mobile platform end-effector and a fixed base plate, connected by three variable length links. Each of the three serial links is coupled to a base plate through a passive revolute joint, and

to the end-effector attachment plate through a nut, which is free to rotate about three perpendicular axes by virtue of a spherical joint coupling. Since the manipulator in the project is intended to be general purpose and to compromise the force sensing and force acting capabilities of the parallel manipulator, it is decided that the base and mobile plates are both of equilateral triangle shape and have the same size. The entire arrangement of attachment points on the mobile and the base plates is made as symmetric as possible to simplify the analysis and operation [11].

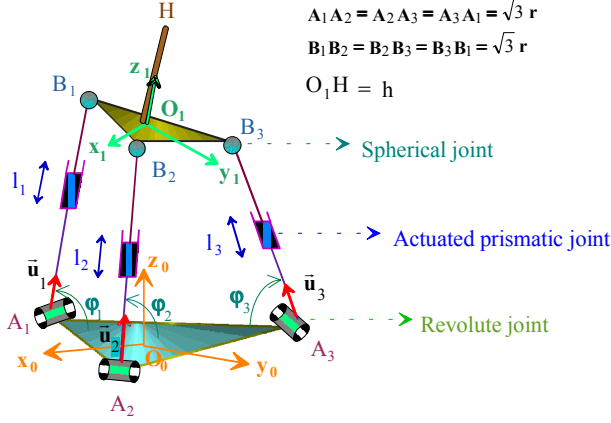


Figure 1. A linear type 3-DOF parallel mechanism

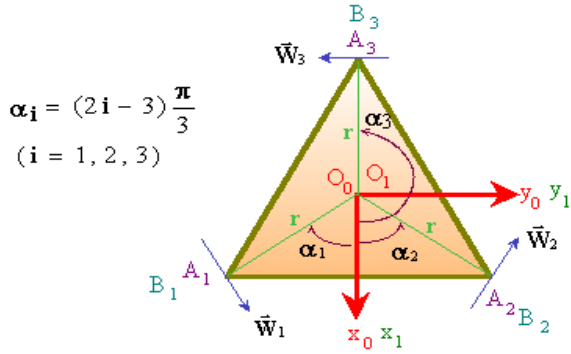


Figure 2. Top view at initial position

This mechanism that has two degrees of orientation freedom (pitch and yaw rotations) and one degree of translation freedom (plunging motion) can provide the necessary flexibility for insertion operations with accuracy.

### B. Notations

Let  $\mathfrak{R}_0$  a fixed coordinate frame ( $\mathbf{O}_0, \bar{x}_0, \bar{y}_0, \bar{z}_0$ ) attached to the center of the base platform,  $\mathfrak{R}_1$  a moving coordinate frame ( $\mathbf{O}_1, \bar{x}_1, \bar{y}_1, \bar{z}_1$ ) attached to center of the mobile platform,  $r$  radius from the center of the base or from the center of the mobile platform,  $\alpha_i$  distribution angle  $i$  ( $i = 1, 2, 3$ ) of the base platform,  $\phi_i$  angle  $i$  ( $i = 1, 2, 3$ ) from the median of the base triangle to the linear link axis  $i$ ,

$l_i$  length of the linear variable link  $i$  ( $i = 1, 2, 3$ ) which is controlled variable,  $h$  length of the cylindrical peg mounted on the end-effector and equal to  $\mathbf{O}_1\mathbf{H}$ ,  $\bar{u}_i$  and  $\bar{w}_i$  unit vectors defined as in Fig. 1 and Fig. 2, and  $\bar{S}_i = \overrightarrow{\mathbf{HB}_i}$  ( $i=1,2,3$ ).

Because only three among the six position and orientation parameters of the mobile platform of this mechanism are independent, the end effector point  $\mathbf{H}$  attached to the mobile platform can be located either by the orientation angles ( $\theta_x, \theta_y$ ) which are pitch and yaw rotations, and the plunge distance  $z = \mathbf{O}_0\mathbf{O}_1$ , or simply by the end effector position ( $X, Y, Z$ ) of the point  $\mathbf{H}$  expressed in the reference frame  $\mathfrak{R}_0$ . There is a strict dependent relationship between ( $z, \theta_x, \theta_y$ ) and ( $X, Y, Z$ ).

As demonstrated in [11], if ( $l_i, \phi_i$ ) ( $i=1,2,3$ ) are well known, ( $\theta_x, \theta_y, z$ ) or ( $X, Y, Z$ ) can be determined in function of ( $l_i, \phi_i$ ) ( $i=1,2,3$ ).

### C. Inverse Kinematics

The inverse kinematics of this parallel mechanism is straightforward and can be stated as follows: *given a desired end-effector orientation ( $\theta_x, \theta_y$ ) and plunge distance  $z$ , or simply given a desired end-effector position ( $X, Y, Z$ ), find a set of input lengths of the linear variable links  $l_i$  ( $i = 1, 2, 3$ ), that will produce the desired results.*

From previous results reported in [11] and for  $i = 1, 2, 3$ , we have

$$l_i = \left\| \overrightarrow{\mathbf{A}_i\mathbf{B}_i} \right\| = \left[ \left( X - r \cos \alpha_i + m_{11}r \cos \alpha_i + m_{12}r \sin \alpha_i - m_{12}h \right)^2 + \left( Y - r \sin \alpha_i + m_{21}r \cos \alpha_i + m_{22}r \sin \alpha_i - m_{23}h \right)^2 + \left( Z + m_{31}r \cos \alpha_i + m_{32}r \sin \alpha_i - m_{33}h \right)^2 \right]^{1/2}. \quad (1)$$

where coefficients  $m_{ij}$  for  $i = 1, 2, 3$  and  $j = 1, 2, 3$ , are function of ( $\theta_x, \theta_y$ ) or of ( $X, Y$ ).

### D. Forward Kinematics

The forward kinematics of the proposed parallel manipulator is much more complicated and can be stated as follows: *given a set of input lengths of the linear variable links  $l_i$  ( $i = 1, 2, 3$ ), find the plunge distance  $z$  and orientation ( $\theta_x, \theta_y$ ) of the tool coordinate frame, or simply find the end-effector position ( $X, Y, Z$ ).*

Again, from previous results reported in [11] and for  $i=1,2,3$  and  $j=1,2,3$ , we have

$$l_i^2 + l_j^2 + l_i l_j \cos \phi_i \cos \phi_j - 2 l_i l_j \sin \phi_i \sin \phi_j - 3r l_i \cos \phi_i - 3r l_j \cos \phi_j = 0. \quad (2)$$

By permuting the indices  $i$  and  $j$  in (2) we can obtain

$$l_1^2 + l_2^2 + l_1 l_2 \cos \varphi_1 \cos \varphi_2 - 2 l_1 l_2 \sin \varphi_1 \sin \varphi_2 - 3 r_1 \cos \varphi_1 - 3 r_2 \cos \varphi_2 = 0, \quad (3)$$

$$l_2^2 + l_3^2 + l_2 l_3 \cos \varphi_2 \cos \varphi_3 - 2 l_2 l_3 \sin \varphi_2 \sin \varphi_3 - 3 r_2 \cos \varphi_2 - 3 r_3 \cos \varphi_3 = 0, \quad (4)$$

$$l_1^2 + l_3^2 + l_1 l_3 \cos \varphi_1 \cos \varphi_3 - 2 l_1 l_3 \sin \varphi_1 \sin \varphi_3 - 3 r_1 \cos \varphi_1 - 3 r_3 \cos \varphi_3 = 0. \quad (5)$$

Simultaneous solution of (3), (4), and (5) is to find  $\varphi_i$  ( $i=1,2,3$ ), given  $\mathbf{l}_i$  ( $i=1,2,3$ ). As reported in [11], an input-output polynomial of degree 4 can be expressed as

$$3l_1^4 t^4 + 12r_1 l_1^3 t^3 - (6l_1^4 + 6l_1^2 l_2^2 + 36r^2 l_1^2) t^2 + 12(l_1^2 + l_2^2) r_1 l_1 t - (l_1^2 - l_2^2)^2 = 0, \quad (6)$$

where  $\mathbf{t} = \cos \varphi_1$  with  $\varphi_1 \neq k\pi$ .

Once  $\mathbf{t}$  is determined from (6), angles  $\varphi_i$  ( $i=1,2,3$ ) can be determined by following formula.

$$\varphi_1 = \cos^{-1}(\mathbf{t}),$$

$$\varphi_2 = \sin^{-1} \left( \frac{l_1^2 + l_2^2 + l_1^2 t^2 - 6r_1 l_1 t}{2l_1 l_2 \sin \varphi_1} \right),$$

and

$$\varphi_3 = \sin^{-1} \left( \frac{(l_2^2 - l_1^2) l_1 \sin \varphi_1}{l_3 (l_2^2 - l_1^2 + 3l_1^2 t^2 - 6r_1 l_1 t)} \right).$$

So, when angles  $\varphi_i$  ( $i=1,2,3$ ) are known for given  $\mathbf{l}_i$ , the end-effector position ( $\mathbf{X}$ ,  $\mathbf{Y}$ ,  $\mathbf{Z}$ ) of the point  $\mathbf{H}$  can be determined in function of  $(\mathbf{l}_i, \varphi_i)$  ( $i=1,2,3$ ), as reported in [11].

### E. Jacobian Matrices

Let define  $\bar{\mathbf{V}}$  as translational velocity of the point  $\mathbf{H}$  and

$\bar{\mathbf{\Omega}}$  angular velocity of the mobile platform, and  $\bar{\mathbf{i}} = \begin{bmatrix} \dot{i}_1 \\ \dot{i}_2 \\ \dot{i}_3 \end{bmatrix}$

actuator velocity vector of the three links. As demonstrated in [11], we have

$$\bar{\mathbf{i}} = \begin{bmatrix} \dot{i}_1 \\ \dot{i}_2 \\ \dot{i}_3 \end{bmatrix} = \mathbf{J}_V \cdot \bar{\mathbf{V}} = \mathbf{J}_\Omega \cdot \bar{\mathbf{\Omega}}, \quad (7)$$

where  $\mathbf{J}_V = [\mathbf{U}] + [\mathbf{S}_U] \cdot ([\mathbf{S}_W]^{-1} \cdot [\mathbf{W}])$ ,

and  $\mathbf{J}_\Omega = [\mathbf{U}] \cdot ([\mathbf{W}]^{-1} \cdot [\mathbf{S}_W]) + [\mathbf{S}_U]$ ,

with  $[\mathbf{U}] = [\bar{u}_1 \quad \bar{u}_2 \quad \bar{u}_3]^T$ ,

$$[\mathbf{S}_U] = [\bar{\mathbf{s}}_1 \wedge \bar{\mathbf{u}}_1 \quad \bar{\mathbf{s}}_2 \wedge \bar{\mathbf{u}}_2 \quad \bar{\mathbf{s}}_3 \wedge \bar{\mathbf{u}}_3]^T,$$

$$[\mathbf{W}] = [\bar{w}_1 \quad \bar{w}_2 \quad \bar{w}_3]^T,$$

$$[\mathbf{S}_W] = [-\bar{\mathbf{s}}_1 \wedge \bar{\mathbf{w}}_1 \quad -\bar{\mathbf{s}}_2 \wedge \bar{\mathbf{w}}_2 \quad -\bar{\mathbf{s}}_3 \wedge \bar{\mathbf{w}}_3]^T.$$

$\mathbf{J}_V$  and  $\mathbf{J}_\Omega$  are 3 by 3 square Jacobian matrices of the parallel mechanism. They represent the mapping between the input rates and the independent output parameters, and will take different forms when different independent parameters are specified.

Equation (7) indicates that three components of the velocity  $\bar{\mathbf{V}}$  are independent parameters, as soon as  $\bar{\mathbf{V}}$  is given, the actuator velocity  $\bar{\mathbf{i}}$  and angular velocity  $\bar{\mathbf{\Omega}}$  will be determined. Similarly, three components of the angular velocity  $\bar{\mathbf{\Omega}}$  can be considered as independent parameters, as soon as  $\bar{\mathbf{\Omega}}$  is given,  $\bar{\mathbf{i}}$  and  $\bar{\mathbf{V}}$  will be determined.

## III. CONTROL SYSTEM

### A. Hybrid Control Algorithm

The kinematic hybrid position/force control system is designed on the basis of the following concepts:

- The manipulator is easily controlled in both programmed autonomous and teleoperation modes. The system can easily switch between these modes or combine them simultaneously.
  - The control system exploits the mechanical properties of the parallel-link mechanism, for example, easy inverse kinematics and difficult inverse statics.
- Taking these concepts into account, the controller is based on the hybrid position/force control loop and the conventional PID scheme is used for the position servos.

The block diagram of the hybrid control scheme is shown in Fig. 5. Commands are generated by applying forces and torques on a fixed base 6-axis force-torque sensor used as a joystick. The referenced signal to be tracked is the joystick signal which is input in base coordinates. The position ( $\mathbf{z}$ ) and orientation ( $\boldsymbol{\theta}_x$ ,  $\boldsymbol{\theta}_y$ ) or simply the position ( $\mathbf{X}$ ,  $\mathbf{Y}$ ,  $\mathbf{Z}$ ) of the end-effector of the parallel manipulator are controlled in the base coordinate frame to ensure stable motion. If the end-effector has no contact with its environment, the velocity of the end-effector should be designated. If the end-effector has contact, it should be provided with compliant motion by using force-torque sensor data, which are compared with the reference signal to get the error signal. This error is then pre-multiplied by a compliance matrix to produce an end-effector command velocity which is transformed to joint coordinates via the Jacobian matrix by using (7), resolved into link speeds by digital integration, and sent to the link position servos. Dead bands are imposed on the data form each of the force-torque sensors to eliminate jitter and drift due to sensor noise.

When no reference signal is applied from the joystick, the manipulator servos on a constant end-effector position, and so maintains positional stability. When moving in free space with no feedback from the end-effector force-torque

sensors, speed is controlled by the joystick signal acting as a Cartesian coordinate rate control input for the manipulator. When contact is made, the joystick signal becomes command force for force control loop making the manipulator naturally compliant. For example, if the end-effector approaches a rigid surface at an angle and a vertical force is imposed via the joystick, the manipulator makes contact with the surface and then rotates so that the end-effector is normal to surface, in order to relieve the moments generated by the oblique reactive contact force. Fig. 3 illustrates this example of compliant motion.

This control method performs remarkably well as a unilateral teleoperation control whose stability is not affected by the time delay causing usually instability in the bilateral teleoperation control.

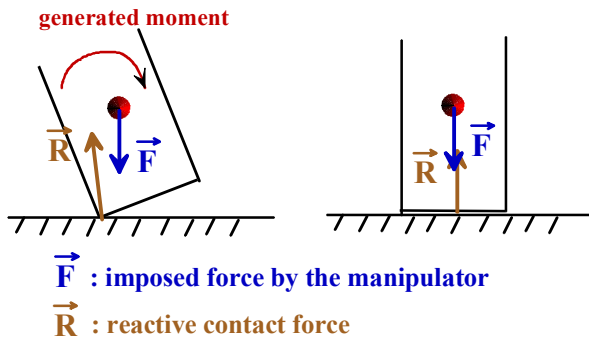


Figure 3. Compliant motion

### B. Control Hardware and Software

TABLE I resumes the kinematic specification of the proposed 3-DOF parallel mechanism illustrated in Fig. 4. The outline of the hardware system is shown in Fig. 6. The whole system consists of 5 subsystems, which are a parallel mechanism, an actuators system, a sensors system, a controller, and a task environment. The components of those subsystems are described below.

1) *Parallel Mechanism*: The three actuated prismatic joints are based on ball-screw system. Each of the three ball-screws is coupled to a base plate through a passive revolute joint, and to the end-effector attachment plate through a nut which is free to rotate about three perpendicular axes by virtue of a spherical joint coupling, which is customized using the THK spherical plain bearing type SA1 from Japan.

2) *Actuators System*: The linear actuator is obtained from the combination of an electric motor and a ball-screw system. Each link is driven by a DC-servomotor 2036U giving a peak rated torque about 0.22[Nm]. The choice of those actuator characteristics is based on the requirement of the load capacity of the end effector about 30N.

3) *Sensors System*: For each link an incremental rotary 5[V] DC encoder with 2500ppr resolution is connected directly to the bottom of each motor to measure the linear displacement of the link. In addition, a joint encoder is

mounted on the trunnion axis at the lower end of each of the three links. Totally, there are 3 encoders that provide the necessary data for the control loop and 3 joint encoders for forward kinematics solution. Also, 3 proximity sensors are mounted on the parallel mechanism to make sure that the mobile platform can find its home position. An optocoupler circuit TLP521-4 is used to protect and isolate control signals between the proximity sensors and the motion controller kit.

For peg-in-hole demonstration, the parallel manipulator will be teleoperated by using the Force/Torque (F/T) sensor as a joystick. Two 6-axis F/T sensors (JR3 model) mounted respectively on the end plate of the manipulator and the base of the joystick are needed. Each F/T sensor has a maximum force capacity of 30[N] in the x and y directions, 50[N] in the z-direction and a maximum torque capacity of 3[Nm].

4) *Controller*: The parallel manipulator can be controlled entirely by software run on an IBM PC Pentium III computer with an input-output (I/O) expansion unit. This PC computer is used as a user interface and to compute in real time the control input.

Data measured from the two F/T sensors are input through two F/T receiver cards model JR3 DSP which plug into 16 bit on the PC ISA bus.

Pulses from the three incremental encoders representing 3 joint positions are input into counter circuit through a motion controller card from Motion Engineering, Inc. (MEI) which plugs into 16 bit on the PC ISA bus. The PC computer via the AT-bus lines reads the encoder pulses. A buffer circuit connects the 3 additional encoders representing 3 revolute joint angles installed on the pin joints at the base plate to an analog-digital A/D converter card model NuDaq-PCI8133. The PC computer performs calculations based on the control algorithm and generates signal to the digital-analog D/A converter built in the MEI card. The analog signals enter the three servo amplifiers model minimotor-BLD 5603/06, which produce output current proportional to the voltages of the input signals. The currents generate motor torques to drive the mechanical links through the ball screws system. The control software has been written in C language using Microsoft Visual C/C++ development package. The controller sampling time is 10ms including the data reading from force torque sensors and three pin joint encoders (forward kinematics is not needed), the solution of the inverse kinematics, Jacobian matrices calculation, and position servo. The values of digital PID control gains are selected using Ziegler-Nichols method to get the best time response with minimum steady state position error and without overshoot or actuator saturation.

Experimentally,  $\mathbf{K}_P = \text{diag}\{\mathbf{K}_{P_i}\}$ ,  $\mathbf{K}_I = \text{diag}\{\mathbf{K}_{I_i}\}$ , and  $\mathbf{K}_D = \text{diag}\{\mathbf{K}_{D_i}\}$ , ( $i = 1,2,3$ ),

where  $\mathbf{K}_{P_i} = 100$ ,  $\mathbf{K}_{I_i} = 1$ , and  $\mathbf{K}_{D_i} = 200$ .

5) *Task Environment*: For the insertion operation, a material of contact object containing a hole is fabricated and a tool (peg) is mounted at the end effector of the

parallel manipulator. Both are made of steel. The peg and the hole are 20mm in diameter and the clearance is 10 $\mu$ m. Chamfer is less than 0.2mm in peg and hole.

The insertion task may consist of 4 following motions:

- Approach the hole chamfer vertically using plunging motion.
- Move along the hole chamfer using pitch and yaw rotations.
- Align the peg to the axis of the hole.
- Insert by applying a constant speed along the hole axis.

In teleoperation mode the human operator can observe the task on TV screen. The outline of experimental setup is shown in Fig. 7.

#### IV. CONCLUSION

In this paper, a hybrid position/force control system applied to a three-degree-of-freedom in parallel actuated manipulator is developed. This allows force control as well as stable position control either in manual or automatic modes. For this, we have presented briefly the geometric and kinematic models of the 3-DOF parallel manipulator, and control system with its control algorithm and mechatronics subsystems. The experimental results show that the implemented control is dexterous and robust both in position and force controls. The manipulator has only 3 DOF, and yet a peg can be inserted into a hole with a 10 $\mu$ m clearance, which is rather difficult to do by a human hand directly.

Since the stability of such unilateral control is not affected by the time delay, this control method is very attractive for space teleoperation from a ground-based control center.

#### ACKNOWLEDGMENT

The author would like to acknowledge the financial support of the Ngee Ann Polytechnic of Singapore, and wishes to express his appreciation to the staff members of Robotics and Automation Development programme of the Mechanical Engineering Division for their helpful discussions.



Figure 4. 3-DOF in-parallel actuated manipulator

#### REFERENCES

- [1] B. Roth, K. J. Waldron, M. Raghavan, "Kinematics of a Hybrid series-Parallel Manipulator System", *ASME Journal of Dynamic Systems, Measurement, and Control*, Vol.111, 1989, pp.211-221.
- [2] C. Reboulet and R. Pigeyre, "Hybrid Control of A 6-DOF In-Parallel Actuated Micro-Manipulator Mounted on a Scara Robot", *International Journal of Robotics and Automation*, Vol.7, No.1, 1992, pp.10-14.
- [3] O. Khatib, "Reduced Effective Inertia in Macro-/Mini-Manipulator Systems", *Robotics Research 5*, Miura H. and Arimoto S., Eds., Cambridge: MIT press, 1990, pp.279-284.
- [4] J. P. Merlet, "Force-Feedback Control of Parallel Manipulators", *Proceedings of the International Conference on Robotics and Automation*, 1988, pp.1484-1489.
- [5] K. M. Lee and D. K. Shah, "Kinematic Analysis of a Three-Degrees-of-Freedom In-Parallel Actuated Manipulator", *Proceedings of the International Conference on Robotics and Automation*, Raleigh, USA, 1987, Vol.1, pp.345-350.
- [6] George H. Pfeundshuh et al.: "Design and Control of 3-DOF In-Parallel Actuated Manipulator". *Proceedings of 1991 IEEE international conference on Robotics and Automation*, Sacramento, California, USA, April 1991.
- [7] Y. Fang and Z. Huang, "Kinematics of a Three-Degree-of-Freedom In-Parallel Actuated Manipulator Mechanism", *Mechanism and Machine Theory*, Vol.32, No.7, pp.789-796, 1997.
- [8] P. Huynh, "Dynamic Modeling of the ARTISAN Macro-/mini-Manipulator", *Postdoctoral report*, Stanford University, Dec. 1993.
- [9] T. Arai, R. Stoughton, J. P. Merlet, "Teleoperator Assisted Hybrid Control for Parallel Link Manipulator and Its Application to Assembly Task", *Proceedings of the Second International Symposium on Measurement and Control in Robotics (ISMCR'92)*, Tsukuba, Japan, Nov. 15-19, 1992, pp.817-822.
- [10] P. Huynh et al., "Symmetric Damping Bilateral Control for Parallel Manipulators", *International Conference on Advanced Robotics (ICAR'97)*, Monterey, CA, USA, July 7-9, 1997.
- [11] P. Huynh et al., "Kinematic Analysis and Mechatronics System Design Of a 3-DOF In-Parallel Actuated Mechanism". *Seventh International Conference on Control, Automation, Robotics and Vision (ICARCV 2002)*, Dec. 2 - 5, 2002, Singapore.

TABLE I. KINEMATIC SPECIFICATION

	Range	Units
Ball-screw stroke	Min: +25 Max: +64	mm
Total length of ball-screw	120	mm
Pitch of ball-screw	2 $\pi$	rad/mm
Length of equilateral triangle	89	mm
Height of tool center point	90	mm
Weight	3	kg
Load capacity	3	kg
DC motor output Max. Torque	0.5	Nm
Encoder resolution	2500	ppr
Workspace volume	0.2	dm <sup>3</sup>
Resolution of motion: Z	11	$\mu$ m
Resolution of motion: X, Y	34	$\mu$ m
Velocity (max) of the end effector	0.013	m/s

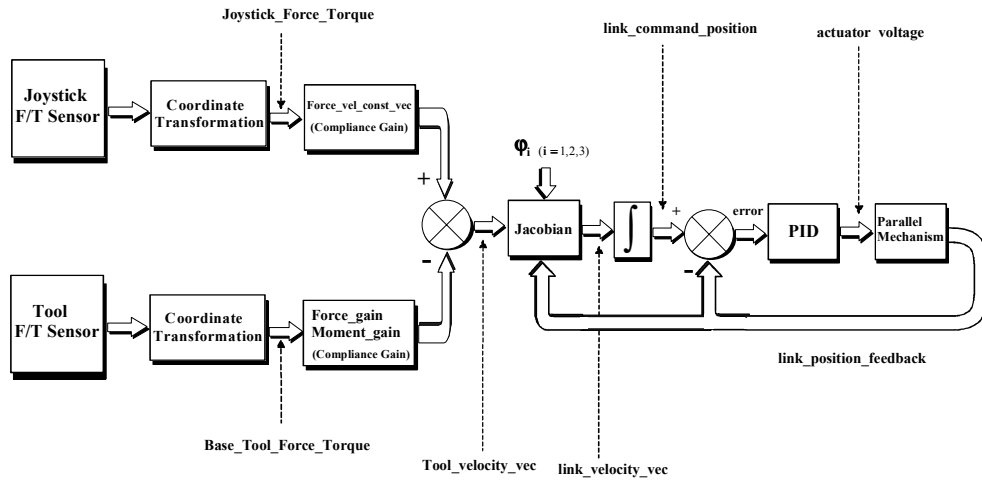


Figure 5. Block diagram of kinematic hybrid control scheme

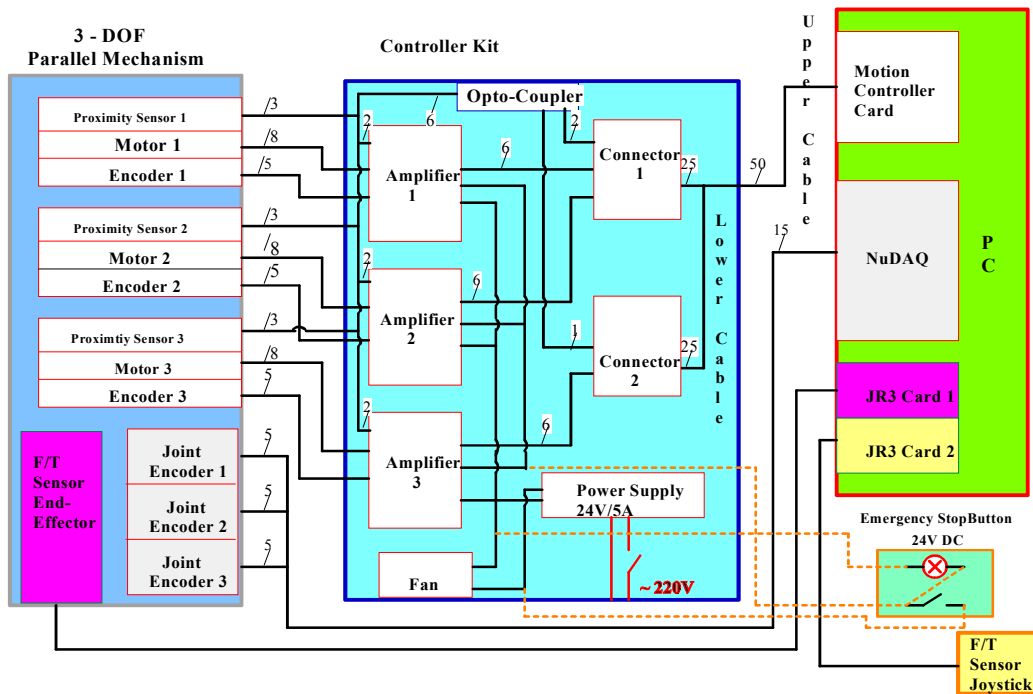


Figure 6. Mechatronics system control of the parallel manipulator

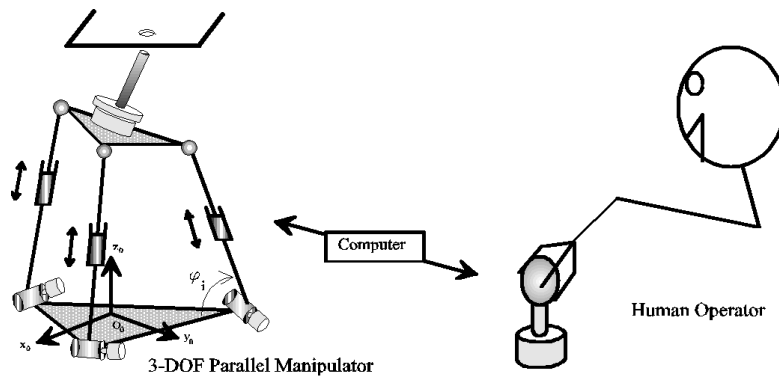


Figure 7. Outline of experimental setup